

Adsorption of 4-aminopyrimidine at the R-AgLAFE/chlorate(VII) interface. Comparison of the adsorption properties of various water activity as well as different surfactants

Marlena Martyna ¹, Alicja Pawlak ¹, Mariusz Grochowski ¹, Aleksandra Bazan-Woźniak ², Robert Pietrzak ², Agnieszka Nosal-Wiercińska ¹

¹ Faculty of Chemistry, Maria Curie-Skłodowska University, Maria Curie-Skłodowska Sq. 3, 20-031 Lublin, Poland

² Faculty of Chemistry, Adam Mickiewicz University in Poznań, Uniwersytetu Poznańskiego 8, 61-614 Poznań, Poland

Corresponding author: marlena.martyna.96@gmail.com (Marlena Martyna)

Abstract: The results of 4-aminopyrimidine (4-APM) impact studies on the double layer parameters at the R-AgLAFE/ chlorates(VII) interface in the solutions with different water activity as well as different properties of the mixed adsorption layer of 4-aminopyrimidine - sodium 1-decanesulfonate (SDS) and 4-aminopyrimidine - hexadecyltrimethylammonium bromide (CTAB) at the electrode/solution interface are discussed. The differential capacity of the double layer (C_d) at the R-AgLAFE/ basic solution interface was measured using the electrochemical impedance spectroscopy. The zero charge potential (E_z) was determined using a streaming electrode, while the surface tension at the zero charge potential (Y_z) was measured using the largest pressure method inside the mercury drop. It was proved that both the 4-aminopyrimidine concentration and water activity have an essential effect on the double layer parameters on the R-AgLAFE/ chlorates(VII) interface. In the studied systems: 4-APM - SDS and 4-APM - CTAB, 4-aminopyrimidine dominance was observed.

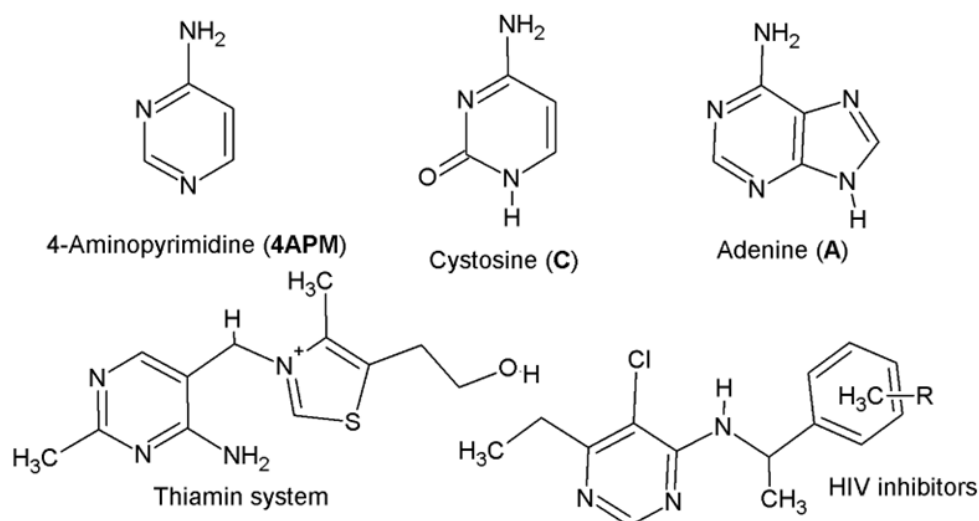
Keywords: 4-aminopyrimidine, SDS, CTAB, R-AgLAFE, specific adsorption

1. Introduction

Recently there has been rapid development in molecular genetics, with the structure and function of both DNA and RNA molecules being the main focus of research. In view of this, it becomes necessary to study the chemical properties of the DNA and RNA precursor molecules (Vaz-Dominguez et al. 2013; Farias et al. 2001). Purines and pyrimidines, the building blocks of nucleic acids, function as cell cycle regulators, energy storage and transporters as well as carriers of cell membrane components and sugars. Pyrimidines are a biologically important class of compounds characterized by the presence of a single six-membered heterocyclic ring and the elements that comprise the rings (most commonly oxygen, nitrogen and sulphur) (Rastogi 2007). Among the known pyrimidine derivatives, 4-aminopyrimidine is mentioned (Scheme 1).

It turns out that the difference in the structure of 4-aminopyrimidine and, for example, cytosine, which is accounted for by the presence of an oxygen atom in cytosine and the $-NH_2$ group, has important implications for the chemical properties and functions of these compounds in the biological systems, especially in the context of their role in DNA and RNA. This is why the research on these compounds is so important for the development of medicine and molecular biology (Raczyńska et al. 2012; Zhou et al. 2017)

Additionally, 4-aminopyrimidine is a compound with potential therapeutic applications and can play a role in the treatment of some diseases. This is a useful building block in the preparation of several anticancer drugs, thiamine and new HIV inhibitors with unknown molecular targets (Raczyńska et al. 2012), and its N-oxides are used in a broad spectrum of antiviral activity (Dueva et



Scheme 1. 4-aminopyrimidine (4-APM) and its biologically active derivatives

al. 2020). It is also a substrate in the enzymatic reactions (Nemeria et al. 2009). In addition, its analogues have shown activity as drugs against Alzheimer's disease, with the ability to cross the blood-brain barrier (Aryan et al. 2016). 4-APM itself possesses good bioavailability as well as potential microbial activity (Venturini Filho et al. 2021). It is also one of the precursors of nucleic acids and occurs in living organisms as part of metabolic processes (Balakrishnan et al. 2012). It can also be synthesized in laboratories for research purposes or as a drug.

This paper presents the results of the 4-APM impact on the double layer parameters at the R-AgLAFE/ chlorates(VII) interface in the solutions with different water activity as well as different properties of the mixed adsorption layer of 4-aminopyrimidine- sodium 1-decanesulfonate and 4-aminopyrimidine - hexadecyltrimethylammonium bromide at the electrode/solution interface.

The mercury electrode is most commonly used in the study of organic compounds due to its very large polarisation range and the advantage of providing reproducible and accurate results (Martin-Yerga et al. 2013; Paleček et al. 2005). An excellent alternative is the cyclically renewable liquid silver amalgam film electrode R-AgLAFE (Nosal-Wiercińska et al. 2021). The design of the sensor ensures a smooth, precise change of the contact surface of the working electrode with the environment being examined, automatic regeneration of the layer of liquid silver amalgam without the contact with atmospheric air, control of the displacement time of the working electrode from the sensor housing to the test solution with preservation of its characteristics acquired during regeneration (Nosal-Wiercińska et al. 2021). Also important in its use is the environmental issue of reducing the toxic mercury required to produce the liquid silver amalgam layer and the generated waste (Nosal-Wiercińska et al. 2021).

The choice of chlorates(VII) solution results from the fact that ClO_4^- ions cause the strongest disruption in the water structure (Nosal-Wiercińska 2010; Nosal-Wiercińska et al. 2010; Gugała-Fekner et al. 2015). The previous studies have shown that the adsorption parameters change along with that of the supporting electrolyte concentration (Nosal-Wiercińska et al. 2017; Nosal-Wiercińska et al. 2015). It was also found that the formation of adsorption equilibria of organic substance-surfactant mixtures is usually dominated by the organic substance. Competitive adsorption between the organic molecules and the surfactants or mixed micelles was also not excluded (Martyna et al. 2022; Nosal-Wiercińska et al. 2018). The aromatic nature of 4-APM indicates a possible adsorption mechanism on the electrode surface (Akyuz et al. 2004). In particular, at its low concentrations in the solution, a flat orientation of the 4-APM molecule on the electrode surface can be expected. On the other hand, the presence of the $-\text{NH}_2$ group suggests complex-forming properties of 4-APM. The results of adsorption studies will be helpful in determination of the mechanism and kinetics of In(III) ion electroreduction in chlorates(VII).

The aim of this study was to demonstrate that both 4-aminopyrimidine concentration and water activity have a significant effect on the parameters of the double layer at the R-AgLAFE/chlorates(VII)

interface. In addition, the influence of the presence of surfactants on the electrode processes was indicated. This will allow the current state of knowledge of electrode processes in which chemical steps play an important role to be expanded and consequently, potentially translated into the targeted therapy related to the identification and understanding of the mechanisms of, for example, controlled drug release.

2. Materials and methods

The chlorates(VII) and 4-aminopyrimidine solutions were prepared from Sigma Aldrich reagents just before the measurements. The concentration of basic electrolyte was $1 \cdot 10^{-3} \text{ mol} \cdot \text{dm}^{-3}$ whereas that of 4-aminopyrimidine ranged from $5 \cdot 10^{-5}$ to $5 \cdot 10^{-3} \text{ mol} \cdot \text{dm}^{-3}$. The supporting electrolyte was made from $1 \text{ mol} \cdot \text{dm}^{-3}$ NaClO_4 and HClO_4 (a few drops of acid were used to dissolve 4-aminopyrimidine because of its tendency towards hydrolysis and after that the whole flask was filled up with the $1 \text{ mol} \cdot \text{dm}^{-3}$ NaClO_4 solution). Both reagents were chosen owing to poor complex-forming properties of ClO_4^- ions and the fact of their small adsorption on the mercury surface. Nitrogen was passed over the solution during the measurements for deaeration. In the measurements sodium 1-decanesulfonate in the range from $1 \cdot 10^{-5}$ to $9 \cdot 10^{-5} \text{ mol} \cdot \text{dm}^{-3}$ and hexadecyltrimethylammonium bromide ranged from $1.5 \cdot 10^{-6}$ to $1.5 \cdot 10^{-5} \text{ mol} \cdot \text{dm}^{-3}$ were used as surfactants.

The adsorption measurements were performed using the AUTOLAB electrochemical analyzer controlled by the GPES software (Version 4.9) (Eco Chemie, Utrecht Netherlands). The cyclically renewable liquid silver amalgam film electrode (R-AgLAFe) with the surface area of 17.25 mm^2 was used as a working electrode and was refreshed before each measurement; the silver/silver chloride electrode (Ag/AgCl, 3 MKCl) was the reference electrode; and the Pt wire was the counter electrode. Soaking the 99.999% purity polycrystalline silver wire in pure mercury (for 2 weeks) has allowed to prepare the silver amalgam film. The silver base (main core) for the amalgam film electrode was made from the 0.5 mm diameter polycrystalline silver wire of 99.999% purity (Alfa Aesar, A. Johnson Matthey Company, Germany). The parameters of measurements were determined in an automatic cell stand mtmanko and were: 3 measuring pulses, 90 ms of measurement time and 750 ms of break time.

The viscosity measurements were performed using the rotational CVO 50 rheometer with the "double gap" measuring system (Bohlin Instruments) and enabled determination of the critical micelle concentration (CMC). The range of the studied concentrations allowed to determine the CMC (for SDS) from the dependence of the solutions viscosity on their concentrations. A rapid change of the system viscosity was observed at the concentration corresponding to CMC (Nosal-Wiercińska et al. 2018).

The differential capacity of the double layer C_d , at the R-AgLAFe/supporting electrolyte interface was determined for the whole polarisation range. The capacity dispersion was tested at different frequencies between 200 and 1000 Hz. The differential capacity curves corresponding to the adsorption equilibrium were obtained as a result of the differential capacitance extrapolation to the zero frequency. According to the assumptions of this procedure, the impedance of the double layer is equivalent to a series of capacitance-resistance combinations and the adsorption rate is diffusion-controlled (Nosal-Wiercińska 2010). The streaming electrode was used to determine the potential of zero charge E_z (Nosal-Wiercińska 2010) with the accuracy of $\pm 0.1 \text{ mV}$. The surface tension at the potential of zero charge Y_z was measured using the method of the highest pressure inside the mercury drop presented by Schiffrin (Nosal-Wiercińska 2010). The surface tension values were determined with the accuracy of $\pm 0.2 \text{ mN} \cdot \text{m}^{-1}$.

3. Results and discussion

3.1. Analysis of experimental data

The course of differential capacity curves on R-AgLAFe in the $1 \text{ mol} \cdot \text{dm}^{-3}$ chlorates(VII) solutions containing $5 \cdot 10^{-5}$ to $5 \cdot 10^{-3} \text{ mol} \cdot \text{dm}^{-3}$ 4-aminopyrimidine pointing out to the change of differential capacity of the double layer at the R-AgLAFe/ chlorates(VII) interface is associated with the presence of 4-aminopyrimidine in the solution (Fig. 1).

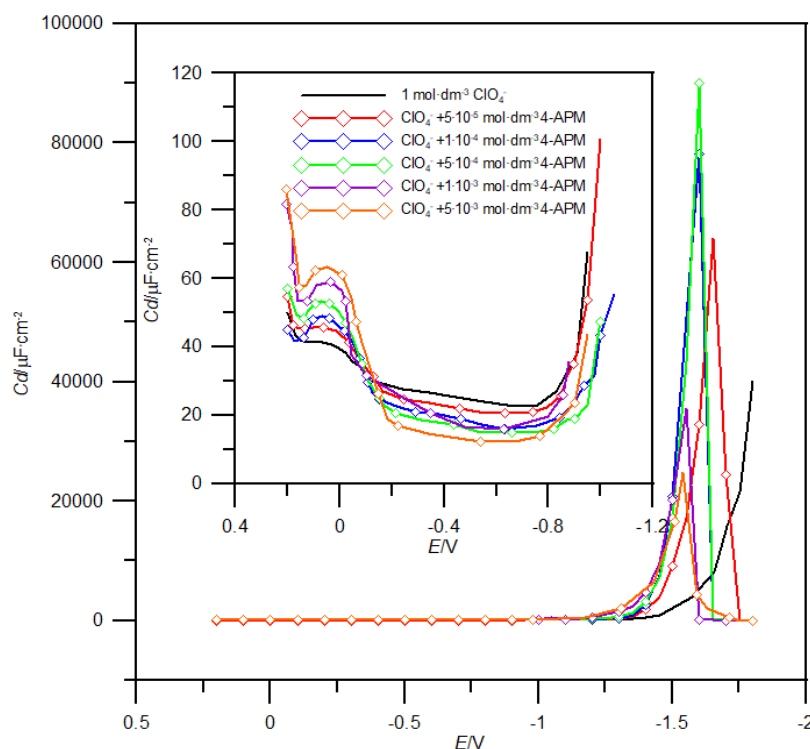


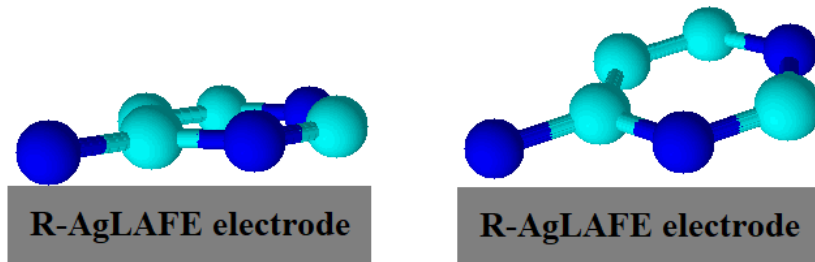
Fig. 1. Differential capacity - potential curves of the double layer of the R-AgLAFe/1 mol·dm⁻³ chlorates(VII) interface with various concentrations of 4-aminopyrimidine presented in the legend

As can be seen in Fig. 1, the addition of 4-APM to the supporting electrolyte solution (1 mol·dm⁻³ chlorates(VII)) caused a significant decrease of the differential capacity in the potential range from -100 mV to -1000 mV. When 4-APM concentration increases, the differential capacity decreases more compared with the supporting electrolyte. This decrease of the double layer differential capacity is related to the strong adsorption of the molecule on the electrode surface (Martyna et al. 2022; Nosal-Wiercińska 2010, Gugala-Fekner 2021).

In contrast, at the potential of about 100 mV, an adsorption peak develops which increases with the increasing 4-APM concentration and is much better defined. The desorption peak, present at the extremely negative potentials (around -1500 mV), increases up to the concentration of 5 · 10⁻⁴ mol·dm⁻³ 4-aminopyrimidine. Subsequent increases in the concentration result in a significant decrease in the desorption peak and a shift towards less negative potentials. This indicates a change in the orientation of the 4-APM molecule on the electrode surface (Skompska 1991; Ikeda et al. 1982). The results of the zero charge potential measurements show a clear shift of E_z values towards positive but only at the smallest 4-APM concentrations ($E_{z, ClO_4^-} = -488\text{mV}$; $E_{z, ClO_4^- + 5 \cdot 10^{-5} APM} = -471\text{mV}$; $E_{z, ClO_4^- + 1 \cdot 10^{-4} APM} = -452\text{mV}$; $E_{z, ClO_4^- + 5 \cdot 10^{-4} APM} = -443\text{mV}$; $E_{z, ClO_4^- + 1 \cdot 10^{-3} APM} = -438\text{mV}$; $E_{z, ClO_4^- + 5 \cdot 10^{-3} APM} = -435\text{mV}$), above the concentration of 5 · 10⁻⁴ mol·dm⁻³ 4-aminopyrimidine these changes are very slight. This behaviour suggests that at smaller concentrations the 4-APM molecules have a flat orientation (Scheme 2) on the electrode surface, facilitating the interactions of the n electrons of the aromatic ring with the electrode surface (Avranas et al. 2000; Kumar et al. 2019; Sotiropoulos et al. 1993).

As opposed, at larger 4-APM concentrations, this interaction becomes weaker as a result of a probably subtle change in the orientation of the molecule from being flat to more oblique. This confirms the earlier suggestions from the image of the capacitance curves. The values of the surface tension Y_z at the zero charge potential ($Y_{z, ClO_4^-} = 485.7\text{mNm}^{-1}$; $Y_{z, ClO_4^- + 5 \cdot 10^{-5} APM} = 482.9\text{mNm}^{-1}$; $Y_{z, ClO_4^- + 1 \cdot 10^{-4} APM} = 481.9\text{mNm}^{-1}$; $Y_{z, ClO_4^- + 5 \cdot 10^{-4} APM} = 481.0\text{mNm}^{-1}$; $Y_{z, ClO_4^- + 1 \cdot 10^{-3} APM} = 480.6\text{mNm}^{-1}$; $Y_{z, ClO_4^- + 5 \cdot 10^{-3} APM} = 479.2\text{mNm}^{-1}$), decrease as proved by the adsorption phenomenon (Batana et al. 1981).

At equal 4-APM concentrations, as the basic electrolyte concentration increases, a decrease in the adsorption peaks in the curves are observed $Cd=f(E)$ and a slight shift towards more positive potentials (Fig. 2).



Scheme 2. Scheme of 4-aminopyrimidine orientation on the R-AgLAFE electrode surface depending on the 4-APM concentration

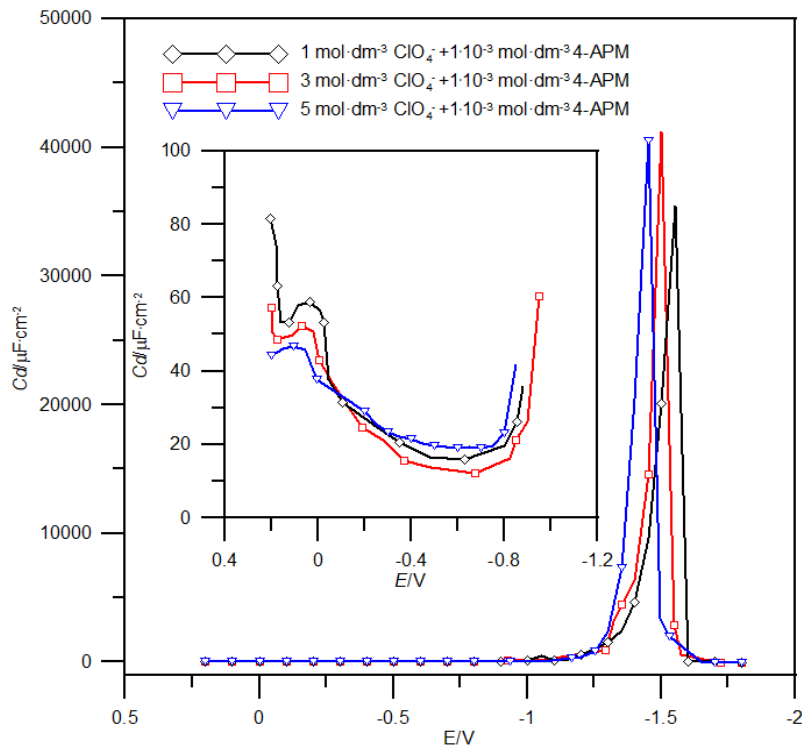


Fig. 2. Differential capacity – potential curves of the double layer of the R-AgLAFE/1-5 mol·dm⁻³ chlorates(VII) interface with the addition of 1·10⁻³ mol·dm⁻³ 4-aminopyrimidine. The concentrations of chlorates(VII) are presented in the legend

The height of the desorption peaks does not change, while the peak potentials shift clearly towards less negative potentials. In the area of strong 4-APM adsorption potentials, a decrease in the water activity results in an effect of increasing differential capacity. Such changes indicate a considerable effect of water on the surface properties of the interface (Nosal-Wiercińska 2010).

For all the examined supporting electrolytes (1, 3 and 5 mol·dm⁻³ chlorates(VII)) concentrations it was concluded that with the increase of 4-APM concentration the zero charge potential E_z values shift towards more negative potentials and the surface tension values at the potential of zero charge E_z decrease. The table includes values for the concentration of 1·10⁻³ mol·dm⁻³ 4-APM (due to the biggest changes in the charge potential E_z values) to better illustrate the effect of increasing water activity (Table 1).

The linear dependencies $E_z=f(C_{adsorbate})$ obtained for all the studied chlorates(VII) concentrations point out to the specific adsorption of adsorbate on the R-AgLAFE electrode (Avranas et al. 2000; Sotiropoulos et al. 1993; Kumar et al. 2019).

The differential capacity curves obtained in the chlorate(VII) solutions containing a fixed amount of 4-aminopyrimidine in the presence of different amounts of the ionic surfactants of sodium 1-decanesulfonate and hexadecyltrimethylammonium bromide are shown in Figures 4 a, b.

Table 1. The potential of zero – charge E_z vs. Ag/AgCl electrode and the surface tension γ_z for E_z of different chlorates(VII) solutions + $1 \cdot 10^{-3} \text{ mol} \cdot \text{dm}^{-3}$ 4-APM systems

chlorates(VII)/ $\text{mol} \cdot \text{dm}^{-3}$ + 4-APM	$-E_z/\text{mV}$	$\gamma_z/\text{m N m}^{-1}$
1.00	477	480.6
3.00	498	473.5
5.00	547	461.6

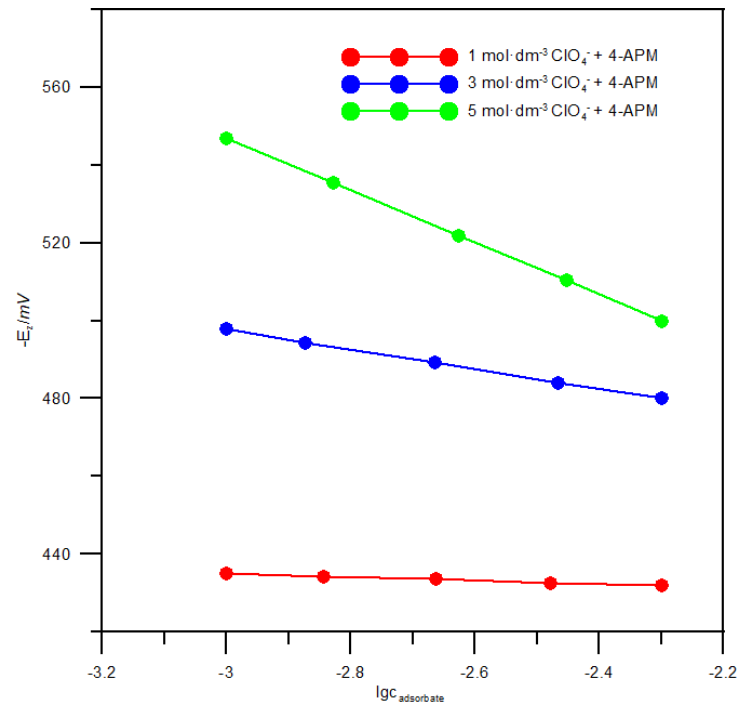


Fig. 3. Linear dependencies $E_z=f(c_{\text{adsorbate}})$ for all the chlorates(VII) concentrations (presented in the legend) with the addition of $1 \cdot 10^{-3} \text{ mol} \cdot \text{dm}^{-3}$ 4-APM

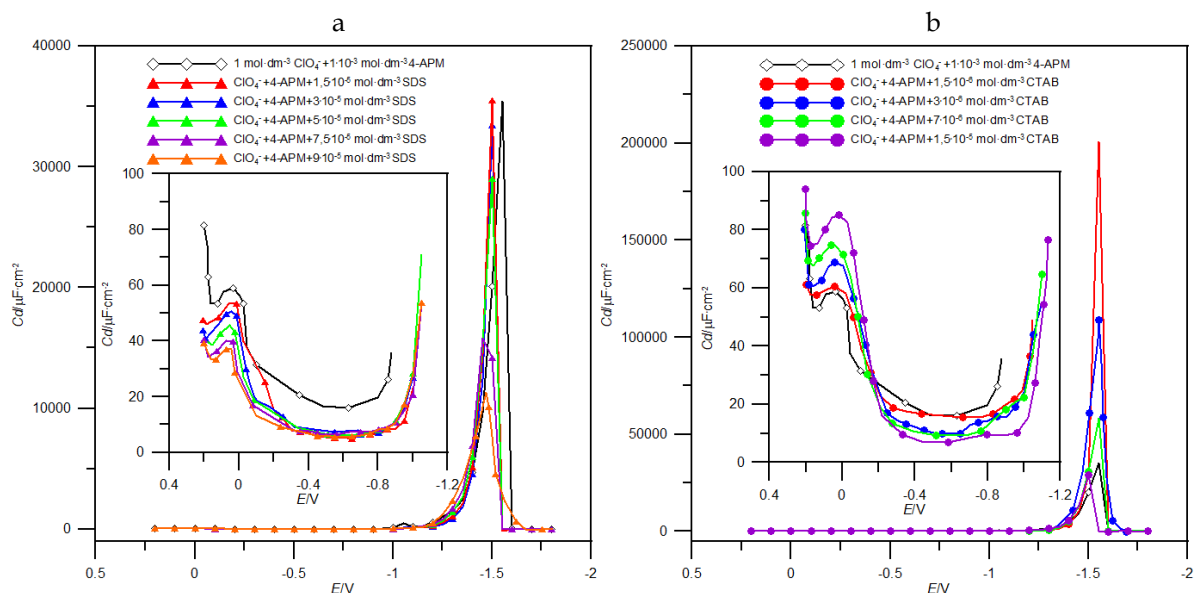


Fig. 4. a. Differential capacity – potential curves of the double layer at the R-AgLAFE/ $1 \text{ mol} \cdot \text{dm}^{-3}$ chlorates(VII) interface with $1 \cdot 10^{-3} \text{ mol} \cdot \text{dm}^{-3}$ 4-aminopyrimidine and with various concentrations of SDS are presented in the legend; b. Differential capacity – potential curves of the double layer at the R-AgLAFE/ $1 \text{ mol} \cdot \text{dm}^{-3}$ chlorates(VII) interface with $1 \cdot 10^{-3} \text{ mol} \cdot \text{dm}^{-3}$ 4-aminopyrimidine and with various concentrations of CTAB are presented in the legend

In the potential region of strong 4-APM adsorption (from -100 mV to -1000 mV), the addition of both SDS and CTAB into the solution containing $1 \cdot 10^{-3} \text{ mol} \cdot \text{dm}^{-3}$ 4-aminopyrimidine always has the effect of reducing the differential capacity relative to the differential capacity of the solution containing the basic electrolyte and 4-APM. In the 4-APM - SDS solutions, a well-developed adsorption peak appears below the characteristic of only 4-APM in the chlorates(VII) solution. The magnitude of this decrease depends on the SDS concentration in the solution. On the other hand, the desorption peak is evidently the resultant of the desorption peak of 4-APM and SDS (Pagac et al. 1998; Kumar et al. 2019) and its parameters change with the changing detergent concentration. It should be emphasized that in the studied system, independently of the SDS concentration, the desorption peak potential corresponding to the maximum 4-APM concentration is about -1500 mV. The effect obtained at this 4-APM concentration and the similar image of the capacitance curves can indicate the dominance of 4-aminopyrimidine in the formation of the adsorption equilibrium in the 4-APM - SDS system in the area of labile adsorption potentials of the used organic substances (Pagac et al. 1998). The possibility of different course of the capacitance curves (adsorption peak area) which indicate the formation of mixed adsorption layers in the 4-APM - SDS system (Pagac et al. 1998) should also be mentioned. The measurement results of the zero charge potential E_z for the 4-APM - SDS system indicate a clear shift in the value of E_z towards less negative ones. It was observed that at the smallest SDS concentrations these shifts are very insignificant. A further increase in the surfactant concentration (particularly above the CMC = $5 \cdot 10^{-5} \text{ mol} \cdot \text{dm}^{-3}$) results in a definite shift towards less negative E_z values. This suggests changes in the interactions between the 4-APM and SDS molecules associated with the competitive adsorption between them (Baars et al. 1994; Gugala-Fekner et al. 2015). There should be also mentioned the possibility of a synergetic effect associated with the formation of mixed micelles in the basic electrolyte solution (Aryan et al. 2016).

Table 2. The potential of zero - charge E_z vs. Ag/AgCl electrode and surface tension Y_z for E_z of $1 \text{ mol} \cdot \text{dm}^{-3}$ chlorates(VII) solutions + $1 \cdot 10^{-3} \text{ mol} \cdot \text{dm}^{-3}$ 4-APM + different SDS surfactant concentration systems.

$10^5 c_{\text{SDS}} / \text{mol} \cdot \text{dm}^{-3}$	$-E_z / \text{mV}$	$Y_z / \text{m N m}^{-1}$
0.0	477	480.6
1.5	477	468.4
3.0	476	464.7
5.0	462	462.8
7.5	450	460.9
9.0	439	458.2

The changes of the surface tension values at the potential of zero charge Y_z decrease (Table 2) are significantly greater in the presence of detergents compared to the basic electrolyte solution containing only 4-APM which is associated with the formation of mixed 4-APM - SDS adsorption layers. However, the interactions of 4-APM molecules and the surfactant resulting in formation of a more or less compact structure of the mixed adsorption layers cannot be excluded (Baars et al. 1994; Gugala-Fekner et al. 2015; Nosal - Wiercińska et al. 2018; Klin et al. 2011).

A markedly different character of the capacitance curves is observed for the 4-aminopyrimidine - hexadecyltrimethylammonium bromide system. The area of strong adsorption, as in the systems discussed above, is characterized by a reduction in the differential capacitance in relation to that of the solution containing the basic electrolyte and 4-APM. The well-developed adsorption peak in the 4-APM - CTAB mixture increases with the increasing CTAB concentration in the basic electrolyte solution (chlorates(VII) + 4 - APM). The desorption peak as the resultant of that of 4-APM and CTAB (Klin et al. 2011; Kumar et al. 2019). changes its parameters with the increasing surfactant concentration. As the surfactant concentration increases, its height decreases markedly. This shape of the curves suggests rather a change in the orientation of the molecules in the electrode adsorption layer. Competitive adsorption between the 4-APM and CTAB molecules should also not be ruled out (Baars et al. 1994; Klin et al. 2011).

Such deviations are confirmed by the changes in the E_z values with the increasing cationic surfactant concentration in the basic electrolyte solution. The shift of E_z values towards the negative

potentials (inversely to SDS) is associated with the adsorption of the 4-APM molecule with the negative pole to the electrode (Brycht et al. 2014). An increase in the surfactant concentration shifts these values slightly. Such an effect and the image of the capacitance curves (with a particular consideration of the desorption peaks) testify to the definite dominance of 4-APM in shaping the adsorption equilibrium in the 4-APM - CTAB system (Gugała-Fekner et al. 2015; Nosal – Wiercińska et al. 2018; Klin et al. 2011). The values of the surface tension γ_z at the zero charge potential (Table 3) decrease for all studied systems as proved by the adsorption phenomenon.

Table 3. The potential of zero - charge E_z vs. Ag/AgCl electrode and the surface tension γ_z for E_z of 1 mol·dm⁻³ chlorates(VII) solutions + 1·10⁻³ mol·dm⁻³ 4-APM + different CTAB surfactant concentration systems.

$10^5 C_{CTAB} / \text{mol} \cdot \text{dm}^{-3}$	$- E_z / \text{mV}$	$\gamma_z / \text{m N} \cdot \text{m}^{-1}$
0.0	477	480.6
0.15	474	476.0
0.30	476	475.5
0.70	477	474.6
1.50	478	479.3

4. Conclusions

The presented experimental studies bring the following conclusions:

- both the 4-aminopyrimidine concentration and water activity have an essential effect on the double layer parameters at the R-AgLAFE/ chlorates(VII) interface;
- specific adsorption of 4-aminopyrimidine on the R-AgLAFE electrode was demonstrated;
- changes of the adsorption parameters in the function of the supporting electrolyte concentration points out the competitive adsorption of 4 - APM and ClO_4^- ions as well as electrostatic interactions between the adsorbate and the water molecules;
- the comparison of different capacitance curves in the applied systems with SDS and CTAB detergents indicates a difference in the adsorption due to the interactions of the coadsorbate molecules;
- changes in the value of the zero charge potential suggest a different adsorption equilibrium in all studied systems;
- a dominance of 4-aminopyrimidine was observed in the 4-APM - SDS and 4 - APM - CTAB systems.

References

- AKYUZ, S., AKYUZ, T., 2004. *FT-IR spectroscopic investigations adsorption of pyrazinamide and 4-aminopyrimidine by clays*. J. Incl. Phenom., 48, 75-80.
- ARYAN, R., BEYZAEL, H., SADEGHI, F., 2016. *Facile Synthesis of Some Novel Tetrasubstituted 2, 4-Diaminopyrimidine Derivatives in Aqueous Glucose Solution as a Fully Green Medium and Promoter*. J. Heterocycl. Chem. 53(6), 1963-1969.
- BALAKRISHNAN, A., GAO, Y., MOORJANI, P., NEMERIA, N. S., TITTMANN, K., JORDAN, F., 2012. *Bifunctionality of the thiamindiphosphate cofactor: Assignment of tautomeric/ionization states of the 4'-aminopyrimidine ring when various intermediates occupy the active sites during the catalysis of yeast pyruvate decarboxylase*. J. Am. Chem. Soc. 134(8), 3873-3885.
- BATANA, A., FILHO, R. R., AVACA, L. A., GONZÁLEZ, E. R., 1981. *Determination of electrical double-layer parameters for the adsorption of neutral molecules at the electrode-solution interface*. J. Comput. Chem. 2(3), 221-224.
- BRYCHT, M., SKRZYPEK, S., NOSAL-WIERCIŃSKA, A., SMARZEWSKA, S., GUZIEJEWSKI, D., CIESIELSKI, W., BURNAT, B., LENIART, A., 2014. *The new application of renewable silver amalgam film electrode for the electrochemical reduction of nitrile, cyazofamid, and its voltammetric determination in the real samples and in a commercial formulation*. Electrochim. Acta. 134, 302-308.
- DUEVA, E. V., TUCHYNSKAYA, K. K., KOZLOVSKAYA, L. I., OSOLODKIN, D. I., SEDENKOVA, K. N., AVERINA, E. B., KARGANOVA, G. G. 2020. *Spectrum of antiviral activity of 4-aminopyrimidine N-oxides against a broad panel of tick-borne encephalitis virus strains*. Antivir. Chem. Chemother. 28, 2040206620943462.

- FARIAS, P. A., WAGENER, A. D. L. R., CASTRO, A. A., 2001. *Ultratrace determination of adenine in the presence of copper by adsorptive stripping voltammetry*. *Talanta*. 55(2), 281-290.
- GUGAŁA-FEKNER, D., NIESZPOREK, J., SIEŃKO, D., 2015. *Adsorption of anionic surfactant at the electrode–NaClO₄ solution interface*. *Monatsh. Chem.* 146, 541-545.
- GUGAŁA-FEKNER, D., 2021. *Adenine adsorption in different pH acetate buffer*. Available at SSRN 3881627.
- IKEDA, O., JIMBO, H., TAMURA, H., 1982. *Adsorption of tetramethylthiourea at the mercury/water interface*. *J. Electroanal. Chem. Interfacial Electrochem.*, 137(1), 127-141.
- KLIN, M., NIESZPOREK, J., SIEŃKO, D., GUGAŁA-FEKNER, D., SABA, J., 2011. *Adsorption of tetramethylthiourea in the presence of cationic detergent at interface electrode/aqueous perchlorate solutions*. *Croat. Chem. Acta*. 84, 475-480.
- KUMAR, D., RUB, M.A., 2019. *Role of cetyltrimethylammonium bromide (CTAB) surfactant micelles on kinetics of [Zn(II)-Gly-Leu]⁺ and ninhydrin*. *J. Mol. Liq.* 274, 639-645.
- MARTÍN-YERGA, D., GONZÁLEZ-GARCÍA, M. B., COSTA-GARCÍA, A., 2013. *Electrochemical determination of mercury: A review*. *Talanta*. 116, 1091-1104.
- MARTYNA, M., GROCHOWSKI, M., URBAN, T., NOSAL-WIERCIŃSKA, A., 2022. *Study of 2-thiocytosine/surfactant adsorption at the R-Ag/LaFe/chlorate (VII) interface—impact of surfactant ionic character*. *Physicochem. Probl. Miner. Process.* 58(2).
- NEMERIA, N. S., CHAKRABORTY, S., BALAKRISHNAN, A., JORDAN, F., 2009. *Reaction mechanisms of thiamin diphosphate enzymes: defining states of ionization and tautomerization of the cofactor at individual steps*. *FEBS J.* 276(9), 2432-2446.
- NOSAL-WIERCIŃSKA, A., 2010. *Adsorption of cystine at mercury/ aqueous solution of chlorate (VII) interface in solutions of different water activity*. *Cent. Europ. J. Chem.* 10, 1290-1300.
- NOSAL-WIERCIŃSKA, A., DALMATA, G., 2010. *Adsorption of methionine at mercury/aqueous solution of chlorate (VII) interface; dependence on the supporting electrolyte concentration*. *Electroanalysis*. 22(17-18), 2081-2086.
- NOSAL-WIERCIŃSKA, A., GROCHOWSKI, M., WIŚNIEWSKA, M., TYSZCZUK-ROTKO, K., YILMAZ, S., YAGMUR, S., YANIK, S., 2015. *Adsorption of selected amino acids at the mercury/aqueous solution interface from the chlorate (VII) and its dependence on the supporting electrolyte concentration*. *Adsorp. Sci. Technol.* 33(6-8), 553-558.
- NOSAL-WIERCIŃSKA, A., WIŚNIEWSKA, M., GROCHOWSKI, M., KALISZCZAK, W., SKRZYPEK, S., BRYCHT, M., FRANUS, W., 2017. *The effect of homocysteine and homocystine protonation on double-layer parameters at the electrode/chlorates (VII) interface*. *Adsorp. Sci. Technol.* 35(5-6), 396-402.
- NOSAL-WIERCIŃSKA, A., KALISZCZAK, W., GROCHOWSKI, M., WIŚNIEWSKA, M., KLEPKA, T., 2018. *Effects of mixed adsorption layers of 6-mercaptopurine–Triton X-100 and 6-mercaptopurine–Tween 80 on the double layer parameters at the mercury/chlorates (VII) interface*. *J. Mol. Liq.* 253, 143-148.
- NOSAL-WIERCIŃSKA, A., MARTYNA, M., GROCHOWSKI, M., BAŚ, B., 2021. *First electrochemical studies on “CAP – PAIR” effect for Bi (III) ion electroreduction in the presence of 2-Thiocytosine on novel cyclically renewable liquid silver amalgam film electrode (R-Ag/LaFe)*. *J. Electrochem. Soc.* 168(6), 066504.
- PAGAC, E. S., PRIEVE, D. C., TILTON, R. D., 1998. *Kinetics and mechanism of cationic surfactant adsorption and coadsorption with cationic polyelectrolytes at the silica–water interface*. *Langmuir*. 14, 2333-2342.
- PALEČEK, E., JELEN, F., 2005. *Electrochemistry of nucleic acids*. In: Paleček E, Scheller F, Wang J (eds) *Perspectives in Bioanalysis*, vol 1. Elsevier, Amsterdam, 73
- RACZYŃSKA, E. D., KOLCZYŃSKA, K., STĘPNIEWSKI, T. M., 2012. *Consequences of one-electron oxidation and one-electron reduction for 4-aminopyrimidine – DFT studies*. *J. Mol. Model.* 18, 3523-3533.
- RASTOGI, S. C., 2007. *Essentials of animal physiology*. New Age International
- SKOMPSCA, M., 1991. *The effect of LiClO₄ concentration on the adsorption behaviour of thiourea at the mercury-ethanolic solution interface*. *J. Electroanal. Chem. Interfacial Electrochem.* 319(1-2), 331-339.
- VAZ-DOMINGUEZ, C., ESCUDERO-ESCRIBANO, M., CUESTA, A., PRIETO-DAPENA, F., CERRILLOS, C., RUEDA, M., 2013. *Electrochemical STM study of the adsorption of adenine on Au (111) electrodes*. *Electrochem. Commun.* 35, 61-64.
- VENTURINI FILHO, E., PINHEIRO, E. M., PINHEIRO, S., GRECO, S. J., 2021. *Aminopyrimidines: Recent synthetic procedures and anticancer activities*. *Tetrahedron*. 92, 132256.
- ZHOU, Z., ZHOU, X., WANG, X., JIANG, B., LI, Y., CHEN, J., XU, J., 2017. *Ultrafast excited-state dynamics of cytosine aza-derivative and analogues*. *J. Phys. Chem.* 121(14), 2780-2789.